Practical Hydrodynamic Optimization of a Trimaran

Chi Yang (AM)[1], **Francis Noblesse** (V)[2] and **Rainald Löhner** (V)[1]

[1]George Mason University
[2]David Taylor Model Basin, NSWC-CD

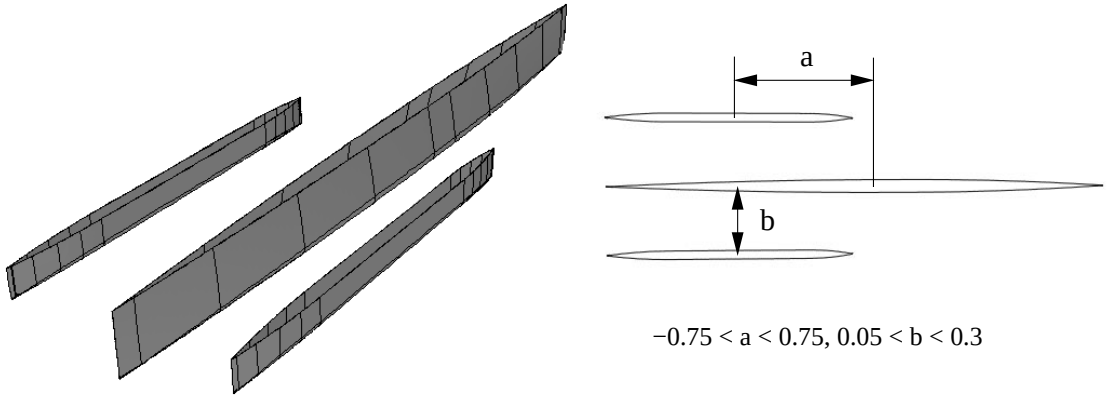

An illustrative application of practical CFD tools to a simple ship design problem is presented. Four methods of analysis — a nonlinear method based on Euler's equations and three linear potential flow methods — are used to determine the optimal location of the outer hulls of a trimaran. The main center hull and the outer hulls of the trimaran are shown in the frontispiece, together with the parameters a and b that define the arrangement of the hulls. The three potential flow methods correspond to a hierarchy of simple approximations based on the Fourier-Kochin representation of ship waves and the slender-ship approximation.

INTRODUCTION

The wave cancellation multihull ship concept considered in Wilson et al. (1993) and Yang et al. (2000) is further examined. The trimaran considered in Wilson et al. (1993), Yang et al. (2000), and the present study consists of a main center hull and two identical outer hulls centered at $(x, y) = (a, \pm b)$ with respect to the center of the waterplane of the main hull. The main center hull of the trimaran has a length $2\,L^c \approx 390'$. The main hull and the outer hulls are depicted in the frontispiece and defined in the Appendix of Yang et al. (2000).

The study considers the elementary design problem of determining the optimal location of the outer hulls with respect to the main center hull, i.e. the optimal values of the two parameters L^X and L^Y, for the purpose of minimizing the wave drag of the trimaran. Four methods of analysis are used and compared to one another and to experimental data. One of the methods is the near-field flow calculation method presented in Löhner et al. (1999) and Yang and Löhner (1998). This method is based on the Euler equations and the nonlinear free-surface boundary condition. The other three methods are linear potential flow methods that correspond to a hierarchy of simple approximations based on the Fourier-Kochin representation of ship waves and the slender-ship approximation given in Noblesse (1983,2001).

HAVELOCK AND FOURIER-KOCHIN REPRESENTATION OF WAVE DRAG

Consider a ship advancing along a straight path, with constant speed $\mathcal{U}$, in calm water of effectively infinite depth and lateral extent. The flow is observed from a Cartesian system of coordinates moving with the ship. The X axis is taken along the path of the ship and points toward the ship bow; i.e., the ship advances in the direction of the positive X axis. The Z axis is vertical and points upward, and the mean free surface is the plane $Z = 0$. The flow appears steady in the translating system of coordinates, and consists of the disturbance flow due to the ship superimposed on a uniform stream opposing the ship's forward speed. The components of the disturbance velocity along the (X, Y, Z)-axes are (U, V, W). Thus, the total velocity is given by $(U - \mathcal{U}, V, W)$. Nondimensional coordinates and velocities are defined in terms of a characteristic length L, taken here as $L = 2\,L^c$, and the ship speed $\mathcal{U}$ as

$$(x\,,y\,,z) = (X,Y,Z)\,/L\,, \quad (u\,,v\,,w) = (U,V,W)\,/\,\mathcal{U}\,.$$

Define the Froude number F and the non-dimensional wave number ν as

$$F = \mathcal{U}/\sqrt{gL}\,, \qquad\qquad \nu = 1/(2F^2)\,,$$

where g is the acceleration of gravity.

The wave drag $R_W = \rho\,\mathcal{U}^2 L^2 C_W$ associated with the wave energy transported by the waves trailing the ship can be determined from the Havelock formula

$$C_W = \frac{\nu}{2\,\pi}\int_{-\infty}^{\infty} \frac{d\beta\;k}{k-\nu}\,(\,S_r^2 + S_i^2\,)\,, \tag{1a}$$

where the wavenumber k is defined in terms of the Fourier variable β by

$$k(\beta) = \nu + \sqrt{\nu^2+\beta^2}\,. \tag{1b}$$

S_r and S_i in (1a) are the real and imaginary parts of the wave spectrum function $S = S(\alpha\,,\beta)$, where α is defined in terms of the Fourier variable β by

$$\alpha(\beta) = \sqrt{k(\beta)}\,/F\,. \tag{1c}$$

The relations (1b) and (1c) follow from the dispersion relation $F^2\alpha^2 = k$ with $k = \sqrt{\alpha^2+\beta^2}$.

The Fourier-Kochin representation of waves given in Noblesse (2001) defines the wave spectrum function S in the Havelock formula (1a) in terms of the velocity distribution at the ship hull surface, or more generally at a boundary surface that surrounds the ship. Specifically, the spectrum function S is defined in terms of distributions of elementary waves over the mean wetted ship hull surface Σ (or a boundary surface Σ that surrounds the ship) and the intersection curve Γ between the surface Σ and the mean free-surface plane $z = 0$:

$$S = \int_\Sigma d\mathcal{A}(\vec{x})\,e^{\,k\,z\,+\,i\,(\,\alpha\,x\,+\,\beta\,y\,)}\,A^\Sigma(\vec{x}) + F^2\int_\Gamma d\mathcal{L}(\vec{x})\,e^{\,i\,(\,\alpha\,x\,+\,\beta\,y\,)}\,A^\Gamma(\vec{x})\,. \tag{2a}$$

Here, $d\mathcal{A}(\vec{x})$ and $d\mathcal{L}(\vec{x})$ respectively stand for the differential elements of area and arc length of Σ and Γ at the integration point $\vec{x} = (x\,,y\,,z \le 0)$. The amplitude functions A^Σ and A^Γ in (2a) are defined in terms of the boundary velocity distribution $\vec{u}$ by

$$A^\Sigma = \vec{u}\cdot\vec{n} + \frac{i\,\alpha}{k}\,(\vec{u}\times\vec{n}\,)^y - \frac{i\,\beta}{k}\,(\vec{u}\times\vec{n}\,)^x\,, \tag{2b}$$

$$A^\Gamma = -(t^y)^2\,\vec{u}\cdot\vec{\nu} + (t^x t^y + \alpha\beta\,/k^2\,)\,\vec{u}\cdot\vec{t}\,. \tag{2c}$$

Here, $\vec{n} = (n^x, n^y, n^z)$ is the unit vector normal to the ship hull surface Σ; $\vec{n}$ points into the fluid domain (i.e. outside the ship). The unit vectors $\vec{t} = (\,t^x, t^y, 0\,)$ and $\vec{\nu} = (-t^y, t^x, 0\,)$ are tangent and normal, respectively, to the ship waterline Γ; $\vec{t}$ is oriented clockwise (looking down) and $\vec{\nu}$ points outside the ship, like $\vec{n}$. Finally, the terms

$$(\vec{u}\times\vec{n}\,)^x = v\,n^z - w\,n^y\,, \qquad (\vec{u}\times\vec{n}\,)^y = w\,n^x - u\,n^z\,,$$

in (2b) are the x and y components of $\vec{u}\times\vec{n}$.

Expressions (2a)–(2c) define the spectrum function S in the Havelock integral (1a) in terms of the normal components $\vec{u}\cdot\vec{n}$ and $\vec{u}\cdot\vec{\nu}$ and the tangential components $\vec{u}\times\vec{n}$ and $\vec{u}\cdot\vec{t}$ of the velocity $\vec{u}$ at the ship hull surface $\Sigma\cup\Gamma$.

APPLICATION TO MULTIHULL SHIPS

If the ship hull surface $\Sigma\cup\Gamma$ consists of N component surfaces, i.e

$$\Sigma = \sum_{j=1}^N \Sigma_j\,, \qquad\qquad \Gamma = \sum_{j=1}^N \Gamma_j\,, \tag{3a}$$

centered at $\vec{x}_j = (x_j\,,y_j\,,z_j)$, the spectrum function S can be expressed as

$$S = \sum_{j=1}^N \Big[\,e^{\,k\,z_j\,+\,i\,(\,\alpha\,x_j\,+\,\beta\,y_j\,)}\,S_j^\Sigma + F^2\,e^{\,i\,(\,\alpha\,x_j\,+\,\beta\,y_j\,)}\,S_j^\Gamma\,\Big]\,, \tag{3b}$$

with

$$S_j^\Sigma = \int_{\Sigma_j} d\mathcal{A}\;A^\Sigma\,e^{\,k\,(\,z\,-\,z_j\,)\,+\,i\,[\,\alpha\,(\,x\,-\,x_j\,)\,+\,\beta\,(\,y\,-\,y_j\,)\,]}\,,$$

$$S_j^\Gamma = \int_{\Gamma_j} d\mathcal{L}\;A^\Gamma\,e^{\,i\,[\,\alpha\,(\,x\,-\,x_j\,)\,+\,\beta\,(\,y\,-\,y_j\,)\,]}\,. \tag{3c}$$

In the particular case of a trimaran consisting of a center hull centered at $(0\,,0\,,0)$ and two identical outer

hulls centered at $(a\,,\pm b\,,0)$, (3b) becomes

$$S = (S_c^\Sigma + F^2 S_c^\Gamma) + e^{i\,a\,\alpha}\,[\,e^{i\,b\,\beta}(S_+^\Sigma + F^2 S_+^\Gamma) + e^{-i\,b\,\beta}(S_-^\Sigma + F^2 S_-^\Gamma)\,]\,.$$

If the outer-hull spectrum functions $S_\pm^\Sigma + F^2 S_\pm^\Gamma$ are assumed to be identical, we have

$$S = (S_c^\Sigma + F^2 S_c^\Gamma) + 2\,\cos(b\,\beta)\,e^{i\,a\,\alpha}(S_o^\Sigma + F^2 S_o^\Gamma)\,.$$

Here, $S_c^\Sigma + F^2 S_c^\Gamma$ and $S_o^\Sigma + F^2 S_o^\Gamma$ stand for the spectrum functions associated with the center hull and an outer hull, respectively.

Define

$$\begin{Bmatrix} S^c \\ S^o \end{Bmatrix} = \begin{Bmatrix} S_r^c + i\,S_i^c \\ S_r^o + i\,S_i^o \end{Bmatrix} = \begin{Bmatrix} S_c^\Sigma + F^2 S_c^\Gamma \\ S_o^\Sigma + F^2 S_o^\Gamma \end{Bmatrix}\,, \qquad (4a)$$

where the spectrum functions S^c and S^o are defined by (2a) in which Σ, Γ are taken as Σ_c, Γ_c or Σ_o, Γ_o. The real and imaginary parts of the spectrum function S are then given by

$$S_r = S_r^c + 2\,\cos(b\,\beta)\,[\,S_r^o\,\cos(a\,\alpha) - S_i^o\,\sin(a\,\alpha)\,]\,,$$

$$S_i = S_i^c + 2\,\cos(b\,\beta)\,[\,S_i^o\,\cos(a\,\alpha) + S_r^o\,\sin(a\,\alpha)\,]\,.$$

These expressions yield

$$S_r^2 + S_i^2 = (S_r^c)^2 + (S_i^c)^2 + 4\cos^2(b\,\beta)\,[\,(S_r^o)^2 + (S_i^o)^2\,] + 4\cos(b\,\beta)\,[\,(S_r^c\,S_r^o + S_i^c\,S_i^o)\,\cos(a\,\alpha) + (S_i^c\,S_r^o - S_r^c\,S_i^o)\,\sin(a\,\alpha)\,]\,.$$

We thus have

$$S_r^2 + S_i^2 = [\,(S_r^c)^2 + (S_i^c)^2\,] + 2\,[\,(S_r^o)^2 + (S_i^o)^2\,] + 4S_*$$

with $\quad S_* = A\,[\cos^2(b\,\beta) - 1/2\,] + [\,A^R\cos(a\,\alpha) + A^I\sin(a\,\alpha)\,]\,\cos(b\,\beta)\,.$

Here, A, A^R and A^I are defined as

$$\begin{Bmatrix} A \\ A^R \\ A^I \end{Bmatrix} = \begin{Bmatrix} (S_r^o)^2 + (S_i^o)^2 \\ S_r^c\,S_r^o + S_i^c\,S_i^o \\ S_i^c\,S_r^o - S_r^c\,S_i^o \end{Bmatrix}\,. \qquad (4b)$$

The wave drag C_W can then be expressed as

$$C_W = C_W^c + 2\,C_W^o + C_W^i\,, \qquad (5a)$$

where C_W^c and C_W^o are given by

$$C_W^c = \frac{\nu}{2\,\pi}\int_{-\infty}^{\infty}\frac{d\beta\;k}{k-\nu}\,[\,(S_r^c)^2 + (S_i^c)^2\,]\,, \qquad (5b)$$

$$C_W^o = \frac{\nu}{2\,\pi}\int_{-\infty}^{\infty}\frac{d\beta\;k}{k-\nu}\,[\,(S_r^o)^2 + (S_i^o)^2\,]\,, \qquad (5c)$$

and represent the wave drags of the center hull and of an outer hull, respectively. The component C_W^i accounts for interference effects and is defined as

$$C_W^i = \frac{2\,\nu}{\pi}\int_{-\infty}^{\infty}\frac{d\beta\;k}{k-\nu}\,[\,\frac{A}{2}\,\cos(2b\,\beta) + A^R\cos(a\,\alpha)\cos(b\,\beta) + A^I\sin(a\,\alpha)\cos(b\,\beta)\,]\,, \qquad (5d)$$

with A, A^R and A^I given by (4b).

FOURIER-KOCHIN REPRESENTATION OF NEAR-FIELD STEADY SHIP WAVES

The Fourier-Kochin representation of waves shows that, within the framework of potential-flow theory, the velocity field $\vec{u}$ generated by a ship can be decomposed as

$$\vec{u} = \vec{u}^{\,W} + \vec{u}^{\,L}\,. \qquad (6a)$$

Here, $\vec{u}^{\,W}$ and $\vec{u}^{\,L}$ respectively represent a wave component and a local component that are associated with the decomposition

$$G = G^W + G^L\,, \qquad (6b)$$

of the Green function G associated with the free-surface boundary condition $w + F^2 u_x = 0$. The wave component $\vec{u}^{\,W}$ is given by a single Fourier integral.

Specifically, the ship hull Σ (which here stands for the center hull Σ_c or an outer hull Σ_o) is divided into a set of patches Σ_p associated with reference points $(x_p\,,y_p\,,z_p \le 0)$ located in the vicinity of Σ_p. The patch reference points $(x_p\,,y_p\,,z_p \le 0)$ attached to the patches Σ_p need not lie on Σ_p. The size of the patches in the x direction is $O(\sigma F^2)$ as required by the function Θ defined by (8).

The wave component $\vec{u}^{\,W}(\vec{\xi})$ at a field point $\vec{\xi} = (\xi\,,\eta\,,\zeta)$ is defined in Yang et al. (2000) as

$$4\pi\begin{Bmatrix} u^W \\ v^W \\ w^W \end{Bmatrix} \approx \int_0^{\beta_c} d\beta\,\frac{e^{\,\zeta\,k}\,\alpha}{k-\nu}\,(1 - \frac{\beta^3}{\beta_c^3})\sum_{p=1}^{N}\Theta_p\begin{Bmatrix} \alpha\,A_p^\alpha \\ \beta\,A_p^\beta \\ k\,A_p^k \end{Bmatrix}\,, \qquad (7)$$

where β_c is a large positive real constant, and α and $k = \sqrt{\alpha^2 + \beta^2}$ are the functions of the Fourier variable β given by (1c) and (1b). Θ_p is defined as

$$\Theta_p = 1 + \tanh(\frac{x_p - \xi}{\sigma\,F^2})\,, \qquad (8)$$

where σ is a positive real constant.

Summation in (7) is performed over all of the N patches Σ_p and line segments Γ_p that represent the surface Σ and waterline Γ, i.e.

$$\Sigma \cup \Gamma = \sum_{p=1}^{N}\,\Sigma_p \cup \Gamma_p\,.$$

Expression (8) yields

$$\Theta_p \to 0 \quad \text{as} \quad (x_p - \xi)/(\sigma F^2) \to -\infty\,.$$

Thus, the contribution of a patch Σ_p to the wave component $\vec{u}^{\,W}$ is negligible at a point $\vec{\xi}$ located at a distance $O(\sigma F^2)$ ahead of the reference point $\vec{x}_p$ attached to Σ_p.

The functions A_p^α, A_p^β, A_p^k in (7) are defined as

$$A_p^\alpha = [\,(S_r^+ + S_r^-)\,C^\xi + (S_i^+ + S_i^-)\,S^\xi\,]\,C^\eta + [\,(S_i^+ - S_i^-)\,C^\xi - (S_r^+ - S_r^-)\,S^\xi\,]\,S^\eta\,, \qquad (9a)$$

$$A_p^\beta = [\,(S_i^+ + S_i^-)\,C^\xi - (S_r^+ + S_r^-)\,S^\xi\,]\,S^\eta + [\,(S_r^+ - S_r^-)\,C^\xi + (S_i^+ - S_i^-)\,S^\xi\,]\,C^\eta\,, \qquad (9b)$$

$$A_p^k = [\,(S_r^+ - S_r^-)\,C^\xi + (S_i^+ - S_i^-)\,S^\xi\,]\,S^\eta - [\,(S_i^+ + S_i^-)\,C^\xi - (S_r^+ + S_r^-)\,S^\xi\,]\,C^\eta\,, \qquad (9c)$$

with $\begin{Bmatrix} C^\xi \\ S^\xi \end{Bmatrix} = \begin{Bmatrix} \cos(\xi\,\alpha) \\ \sin(\xi\,\alpha) \end{Bmatrix}$ and $\begin{Bmatrix} C^\eta \\ S^\eta \end{Bmatrix} = \begin{Bmatrix} \cos(\eta\,\beta) \\ \sin(\eta\,\beta) \end{Bmatrix}$.

Furthermore, $S_r^\pm$ and $S_i^\pm$ in (9a)–(9c) are defined as

$$S_r^\pm = S_p^{\,r}(\alpha\,,\pm\beta)\,, \qquad S_i^\pm = S_p^{\,i}(\alpha\,,\pm\beta)\,, \qquad (10a)$$

where $S_p^{\,r}$ and $S_p^{\,i}$ are the real and imaginary parts of the spectrum function $S_p(\alpha\,,\beta)$ associated with the patch Σ_p. The spectrum function S_p is given by distributions of elementary waves over $\Sigma_p \cup \Gamma_p$. Specifically, (2a) yields

$$S_p = \int_{\Sigma_p} d\mathcal{A}(\vec{x})\, e^{\,k\,z\,+\,i\,(\,\alpha\,x\,+\,\beta\,y\,)}\, A^\Sigma(\vec{x}) + F^2 \int_{\Gamma_p} d\mathcal{L}(\vec{x})\, e^{\,i\,(\,\alpha\,x\,+\,\beta\,y\,)}\, A^\Gamma(\vec{x})\,. \qquad (10b)$$

The amplitude functions A^Σ and A^Γ are defined by (2b) and (2c).

At a distance $O(\sigma F^2)$ behind the ship, (8) yields $\Theta_p \approx 2$ and the foregoing representation of the wave component $\vec{u}^{\,W}$ can be simplified as in Yang et al. (2000). This simplified representation, which does not require subdivision of the ship hull (or more generally boundary surface) $\Sigma \cup \Gamma$ into patches $\Sigma_p \cup \Gamma_p$, is used in Yang et al. (2000) to extend a near-field flow past a ship into a far-field region located entirely behind the ship. The more general representation of $\vec{u}^{\,W}$ given here, on the other hand, is valid in the entire flow domain, and thus can be used to compute near-field waves.

SLENDER-SHIP APPROXIMATION

The slender-ship approximation given in Noblesse (1983,2001) defines the velocity field $\vec{u}(\vec{\xi})$ generated by a ship explicitly in terms of the speed and hull form of the ship:

$$\vec{u}(\vec{\xi}) = \int_\Sigma d\mathcal{A}(\vec{x})\, n^x(\vec{x})\, \nabla_\xi G(\vec{\xi},\vec{x}) + F^2 \int_\Gamma d\mathcal{L}(\vec{x})\, [\,n^x(\vec{x})\,]^2\, t^y(\vec{x})\, \nabla_\xi G(\vec{\xi},\vec{x})\,. \qquad (11)$$

The slender-ship approximation (11) may be regarded as a generalization of the Michell thin-ship approximation. Specifically, the Michell approximation differs from (11) in that it defines $\vec{u}$ in terms of a distribution of sources, with strength $2\,n^x$, over the ship centerplane $y = 0$ in lieu of a distribution of sources of strength n^x over the port and starboard sides of the actual ship surface Σ. In addition, Michell's approximation has no distribution of sources around the waterline Γ.

The slender-ship approximation to the wave component $\vec{u}^{\,W}$ in the decomposition (6a) is given by the Fourier-Kochin representation defined by (7)-(10b) with the amplitude functions A^Σ and A^Γ in (10b) taken as

$$A^\Sigma = n^x\,, \qquad A^\Gamma = (n^x)^2\, t^y\,. \qquad (12)$$

The local component $\vec{u}^{\,L}$ can be effectively evaluated using (11) with the Green function G taken as the very simple analytical approximation to the local component G^L defined in Noblesse (2001) as

$$4\,\pi\,G^L \approx -1/r + 1/r' - 2/r''\,, \qquad (13)$$

with

$$\begin{Bmatrix} r \\ r' \\ r'' \end{Bmatrix} = \begin{Bmatrix} \sqrt{(x-\xi)^2 + (y-\eta)^2 + (z-\zeta)^2} \\ \sqrt{(x-\xi)^2 + (y-\eta)^2 + (z+\zeta)^2} \\ \sqrt{(x-\xi)^2 + (y-\eta)^2 + (z+\zeta-F^2)^2} \end{Bmatrix}.$$

The approximation (13) yields

$$4\,\pi\,G^L \approx -1/r + 1/r' \quad \text{if} \quad r'/F^2 \ll 1\,,$$

$$4\,\pi\,G^L \approx -1/r - 1/r' \quad \text{if} \quad r'/F^2 \gg 1\,,$$

in accordance with the free-surface boundary condition $w + F^2 u_x = 0$.

FOUR METHODS OF ANALYSIS

The wave-drag coefficient C_W defined by (5a)–(5d), (4a) and (4b) accounts for interference effects of the far-field waves generated by the center hull and the two outer hulls. The spectrum functions S^c and S^o in (4a) and (4b) are defined by (2a)–(2c) in terms of the normal and tangential components of the velocity distributions at the center hull Σ_c and the outer hulls Σ_o. The velocity distributions $\vec{u}$ at Σ_c and Σ_o are affected by near-field flow interactions between the center hull and the outer hulls. Thus, the wave drag C_W defined by (5a)–(5d), (4a), (4b) and (2a)–(2c) account for both far-field wave-interference effects and near-field flow interactions.

Evaluation of the wave drag C_W requires evaluation of the near-field velocity distribution $\vec{u}$ at Σ_c and Σ_o for a range of values of the Froude number F and of the parameters a and b that define the location of the outer

hull. This computational task is daunting using typical calculation methods but can actually be easily performed using the slender-ship approximation. Specifically, a single-loop set of computations of the wave drag C_W associated with the slender-ship approximation to the near-field velocity distribution at Σ_c and Σ_o for 4 values of the Froude number, 61 values of a and 26 values of b, corresponding to $4 \times 61 \times 26 = 6,344$ near-field flow calculations (using 11,525 panels to approximate the three hulls) requires 18 hours of CPU time using an SGI origin 2000 with 4 processors. This approach is identified as method 3 hereafter.

Considerable simplifications are obtained if near-field flow interactions are ignored, i.e. if the velocity distribution at the center hull Σ_c is evaluated for the center hull alone (i.e. without the two outer hulls) and the velocity distribution at an outer hull is similarly evaluated for the outer hull alone (i.e. without the center hull and the other outer hull). This approximation, which accounts for far-field wave interference effects but neglects near-field flow interactions, only requires two near-field flow evaluations (one for the center hull, and one for an outer hull) per Froude number, a task that can easily be performed using existing calculation methods. The spectrum functions S^c and S^o defined by (2a)–(2c) and the related functions A, A^R and A^I given by (4b) and (4a) similarly need be evaluated only once per Froude number. The spectrum functions S^c and S^o, like the velocity distributions at the three hulls, are independent of the parameters a and b, which only appear in (5d), within the "negligible near-field interaction" approximation.

Thus, this approximation – identified as method 2 hereafter – effectively uncouples the outer-hull location parameters $(a\,,b)$ and near-field flow calculations. For the purpose of estimating the importance of near-field flow interactions upon the wave drag C_W, the near-field velocity distribution is evaluated here using the slender-ship approximation already used in method 3. Thus, the slender-ship approximation is used to evaluate the near-field flow in both method 2 and method 3. Comparison of methods 2 and 3 provides insight into the importance of near-field flow interaction effects.

Insight into the importance of using a sophisticated near-field flow calculation method can be gained by comparing method 2 and method 1, which corresponds to the zeroth-order slender-ship approximation in Noblesse (1983) and to the trivial approximation

$$A^\Sigma = n^x\,, \qquad\qquad A^\Gamma = (n^x)^2\,t^y\,,$$

in (2b) and (2c). Thus, no near-field flow calculation is required in this simplest approximation. Indeed, the zeroth-order slender-ship approximation is associated with the trivial approximations $\vec{u} \times \vec{n} = 0$ and $\vec{u} \cdot \vec{t} = 0$ for the tangential components of the velocity $\vec{u}$ at the ship hull Σ and waterline Γ, as previously explained.

Methods 1, 2, and 3 are based on the Fourier-Kochin representation of ship waves, i.e. on linear potential flow, and the further simplification associated with the slender-ship approximation. Thus, even method 3 only accounts for effects of near-field flow interactions in an approximate manner. However, near-field flow interactions are fully taken into account in the near-field flow calculation method presented in Löhner et al. (1999) and Yang and Löhner (1998), which is based on the Euler equations and the nonlinear free-surface boundary condition. This method is identified as method 4.

RESULTS OF OPTIMIZATION STUDY

Fig. 1 depicts the experimental values of the residuary drag coefficient C_R given in Wilson et al. (1993) and the corresponding predictions of the wave-drag coefficient C_W given by methods 1, 2, 3, and 4 for the four hull arrangements considered in Wilson et al. (1993). These hull arrangements correspond to $a = -0.128, -0.205, -0.256, -0.385$, and $b = 0.136$ (for all four cases). The left column in Fig. 1 compares C_R and C_W predicted by methods 1 and 2. The right column shows C_R and C_W given by methods 2 and 3, and by method 4 at $F = 0.25\,, 0.3\,, 0.4\,, 0.5$. In Fig. 1, and in all other figures, the measured residuary-drag coefficient C_R and the computed wave-drag coefficient C_W are nondimensionalized in terms of the surface area of the wetted hull, in the usual fashion, as follows,

$$C_R = \frac{R_R}{\frac{1}{2}\rho\,\mathcal{U}^2 S}\,, \quad C_W = \frac{R_W}{\frac{1}{2}\rho\,\mathcal{U}^2 S}\,,$$

Differences between the values of C_W predicted by methods 1 and 2 (left column) and between methods 2 and 3 (right column) are fairly small. These three methods yield values of C_W that are in fair agreement with the experimental values of C_R. In particular, the variation of C_R with respect to the Froude number F is well captured by the theory. The values of C_W given by method 4 at $F = 0.25\,, 0.3\,, 0.4\,, 0.5$ are in even better agreement with C_R on the whole, and are in fairly good agreement with C_W predicted by methods 2 and 3.

Figs. 2a and 2b compare the values of C_W given by methods 1, 2, 3 for two Froude numbers, $F = 0.5$ and $F = 0.3$, and for hull arrangements within the range

$$-0.75 \le a \le 0.75\,, \qquad 0.05 \le b \le 0.3\,. \qquad (14)$$

For $a = 0.75$, the sterns of the outer hulls are aligned with the bow of the main center hull; similarly, the bows of the outer hulls are aligned with the stern of the center hull if $a = -0.75$. The contour plots of $C_W(a\,,b)$ depicted in Figs. 2a and 2b are based on calculations

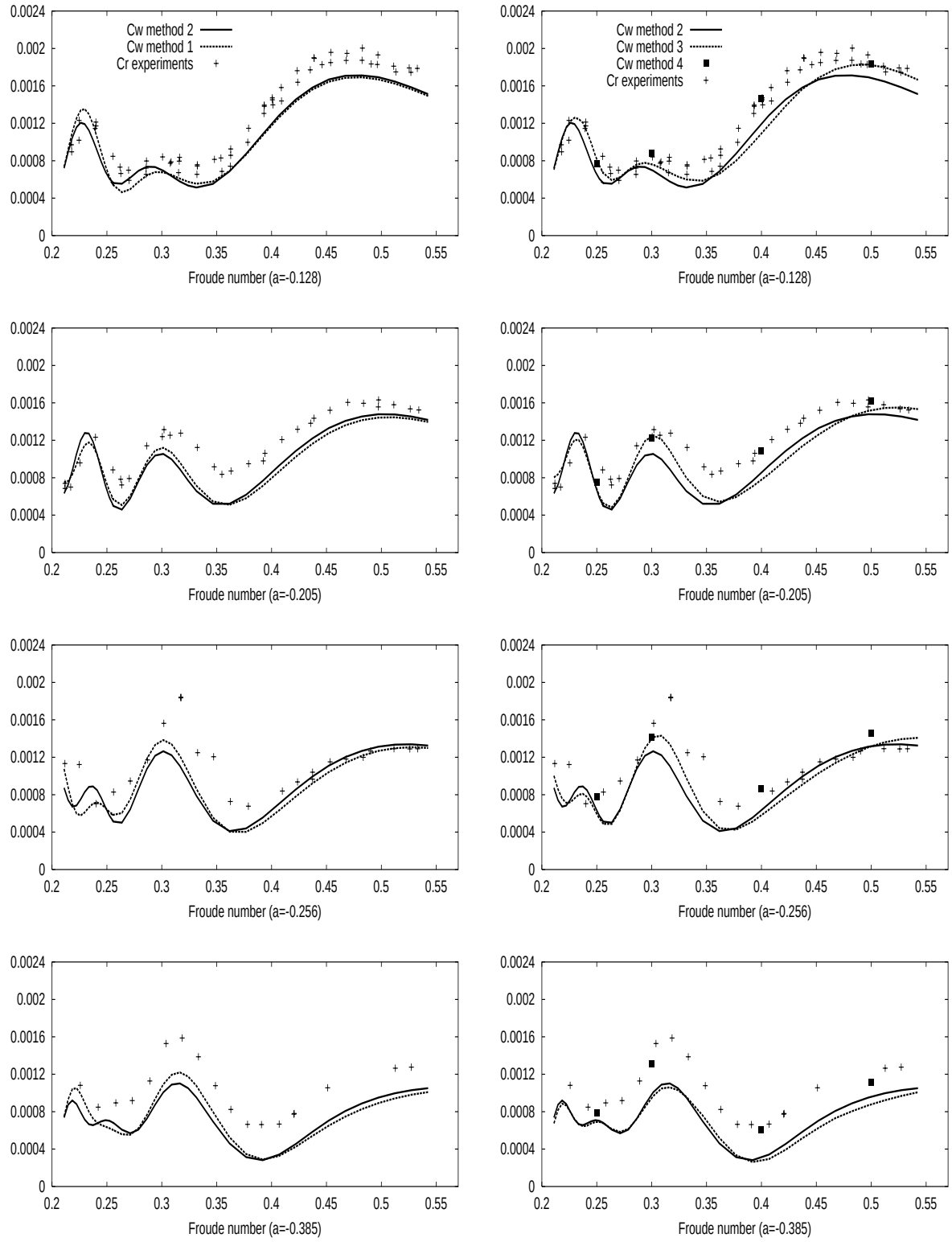

Fig. 1. Experimental residuary drag coefficient and wave drag coefficient calculated using methods 1,2,3,4 for the four hull arrangements considered in Wilson et al. (1993)

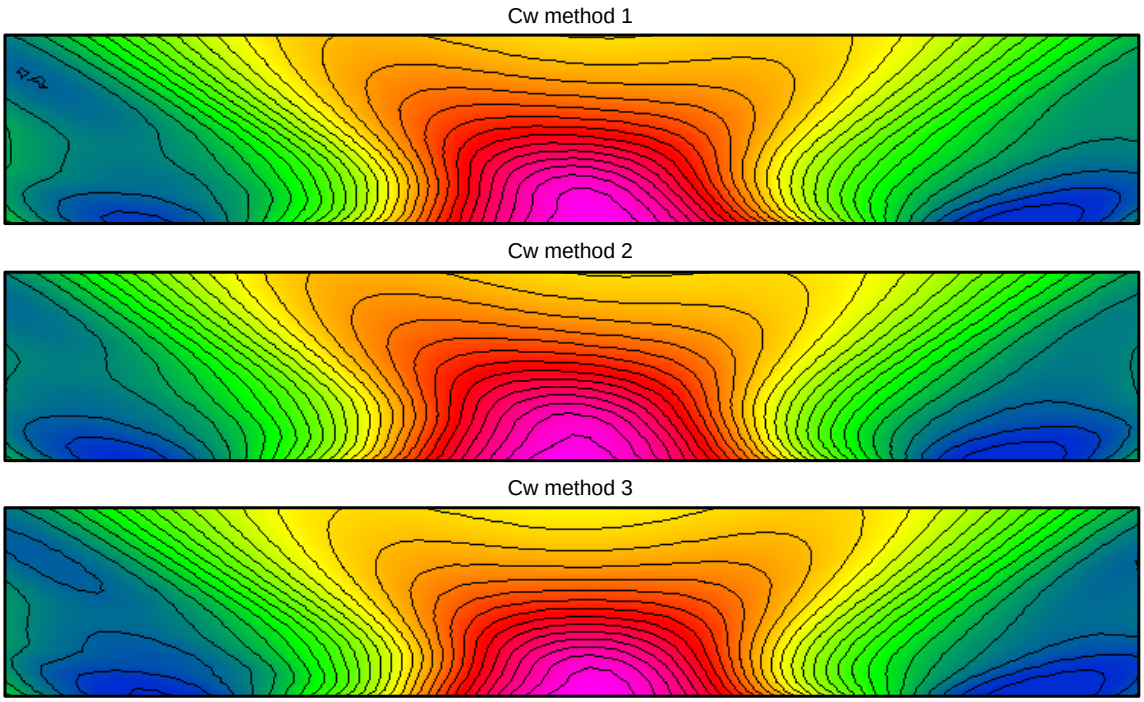

Fig. 2a. Contour plots of wave drag coefficient $C_W(a,\, b)$ predicted by methods 1,2,3 for F=0.5
$(-0.75 \leq a \leq 0.75\,, \quad 0.05 \leq b \leq 0.3)$

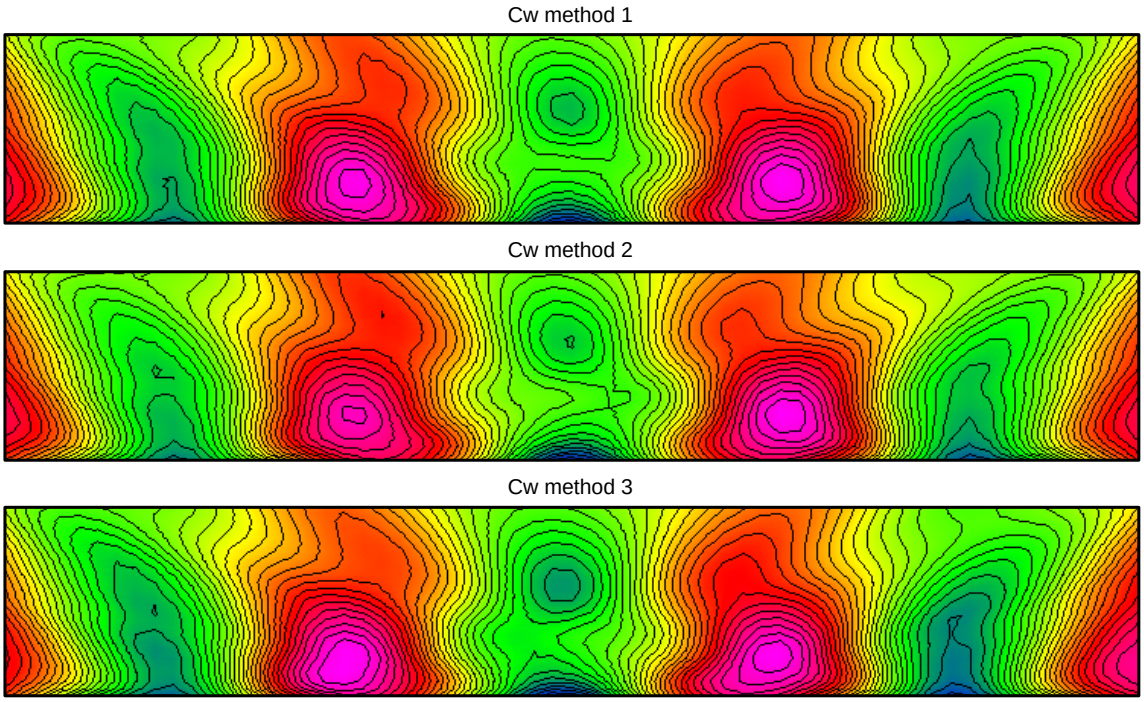

Fig. 2b. Contour plots of wave drag coefficient $C_W(a,\, b)$ predicted by methods 1,2,3 for F=0.3
$(-0.75 \leq a \leq 0.75\,, \quad 0.05 \leq b \leq 0.3)$

for increments in the values of the outer-hull location parameters a and b equal to $\Delta a = 0.025$ and $\Delta b = 0.01$. Thus, the contour plots in Figs. 2a and 2b correspond to evaluations of C_W using methods 1, 2, 3 for 2 values of the Froude number F, 61 values of a and 26 values of b, i.e. $3 \times 2 \times 61 \times 26 = 9,516$ evaluations. Results similar to those depicted in Figs. 2a and 2b are given in Yang et al. (2000) for two more Froude numbers (for $F = 0.4$ and $F = 0.25$). Lowest values of C_W, corresponding to best hull arrangements, are indicated in blue, and highest values of C_W, i.e. worst hull arrangements, are indicated in red. Figs. 2a and 2b, and the additional results given in Yang et al. (2000), indicate that methods 1, 2, and 3 predict best (blue regions, which appear dark in the black and white print-out) and worst (red regions, which appear gray in the black and white print-out) hull arrangements that are in fairly good agreement.

The comparison, presented in Yang et al. (2000), of the values of the wave-drag coefficient C_W obtained using methods 1, 2, 3, 4 for the three best hull arrangements, i.e. for $(a_k\,, b_k)$ with $k = 1\,, 2\,, 3$, predicted by method 2 shows that, although the values of C_W predicted by methods 1, 2, 3, 4 are not identical, these four methods yield $C_1^w \leq C_2^w \leq C_3^w$. These results and the results shown in Figs. 1 and 2a,b of the present study indicate that methods 1 and 2, which are computationally more efficient than methods 3 and 4, may be used for the purpose of determining optimal arrangements of the outer hulls. Method 2 is used here to further study the best and worst outer-hull arrangements.

Fig. 3 shows the variation of the wave-drag coefficient $C_W(a\,, b)$ predicted by method 2 within the region (14) with $\Delta a = 0.025$ and $\Delta b = 0.01$ (as in Figs. 2a and 2b) for 10 values of the Froude number F. Thus, Fig. 3 presents the result of $61 \times 26 \times 10 = 15,860$ evaluations of C_W. As in Figs. 2a,b, lowest and highest values of C_W, i.e. best and worst hull arrangements, correspond to blue and red regions in Fig. 3.

Fig. 4 depicts the variation — within the region (14) considered in Fig. 3 — of the average wave-drag coefficient $\overline{C_W}$ defined as

$$\overline{C_W} = \frac{1}{38} \sum_{i=1}^{38} C_W(F_i)\,.$$

The coefficient $\overline{C_W}$ is the average of the wave-drag coefficient C_W for 38 values F_i of the Froude number F within the range

$$F_1 = 0.2147 \leq F_i \leq F_{38} = 0.5426\,.$$

The contour plot of the coefficient $\overline{C_W}(a\,, b)$ shown in Fig. 4 indicates that, within the region

$$-0.75 \leq a \leq 0.75\,, \qquad 0.1 \leq b \leq 0.3\,, \qquad (15)$$

the optimal hull arrangement for the speed range $F_1 \leq F \leq F_{38}$ is approximately

$$a = 0.575\,, \qquad b = 0.11\,.$$

Fig. 4 presents the result of $61 \times 26 \times 38 = 60,268$ evaluations of C_W.

Fig. 5 depicts the variations, with respect to the Froude number F, of the "no-interference wave-drag coefficient" $C_W^c + 2\,C_W^o$, and of the wave-drag coefficients C_W^{best} and C_W^{worst} associated with the best and worst hull arrangements found (using method 2) within the region (15). Fig. 5 also shows the wave-drag curve $C_W^{optml}(F)$ for the optimal hull arrangement $(a = 0.575\,, b = 0.11)$ previously determined from Fig. 4. The wave-drag curve $C_W^{optml}(F)$ corresponds to a hull arrangement that remains fixed over the entire speed range, while the curves $C_W^{best}(F)$ and $C_W^{worst}(F)$ are associated with hull arrangements that vary with speed. Thus, Fig. 5 shows that we have

$$C_W^{best} \leq C_W^{optml} \leq C_W^{worst}\,,$$

as expected.

The large differences between C_W^{worst} and C_W^{best} apparent in Fig. 5 demonstrate the importance of selecting favorable hull arrangements. Indeed, Fig. 5 shows that the ratio C_W^{worst}/C_W^{best} approximately varies between 2 and 6 within the speed range considered. Fig. 5 also shows that the wave-drag curve $C_W^{optml}(F)$ is significantly lower than the curve $C_W^{worst}(F)$ corresponding to the worst hull arrangements, and even the curve corresponding to the no-interference wave drag $C_W^c + 2\,C_W^o$, over most of the speed range. In fact, the curve $C_W^{optml}(F)$ is remarkably close to the curve $C_W^{best}(F)$, corresponding to the best hull arrangement at every speed, over a broad speed range.

Fig. 6 depicts the experimental values of C_R given in Wilson et al. (1993) for four hull arrangements and the wave-drag coefficients C_W^{best} and C_W^{optml} given by method 2. Fig. 6 also shows the values of the wave-drag coefficient C_W given by method 4 (Euler equations with nonlinear free-surface boundary condition) for the optimal hull arrangement $(a = 0.575\,, b = 0.11)$ obtained using method 2. Although appreciable differences exist between the values of C_W given by methods 4 and method 2, these two methods predict consistent variations of the wave drag with respect to ship speed, as was previously observed in Fig. 1.

Finally, Fig. 7 depicts the wave patterns given by method 4 for the best (top) and worst (bottom) hull arrangements at $F = 0.4069$. The wave pattern for the optimal arrangement $(a = 0.575\,, b = 0.11)$ determined from Fig. 4 is also shown in Fig. 7 (center). Wave-interference effects are clearly apparent in this figure.

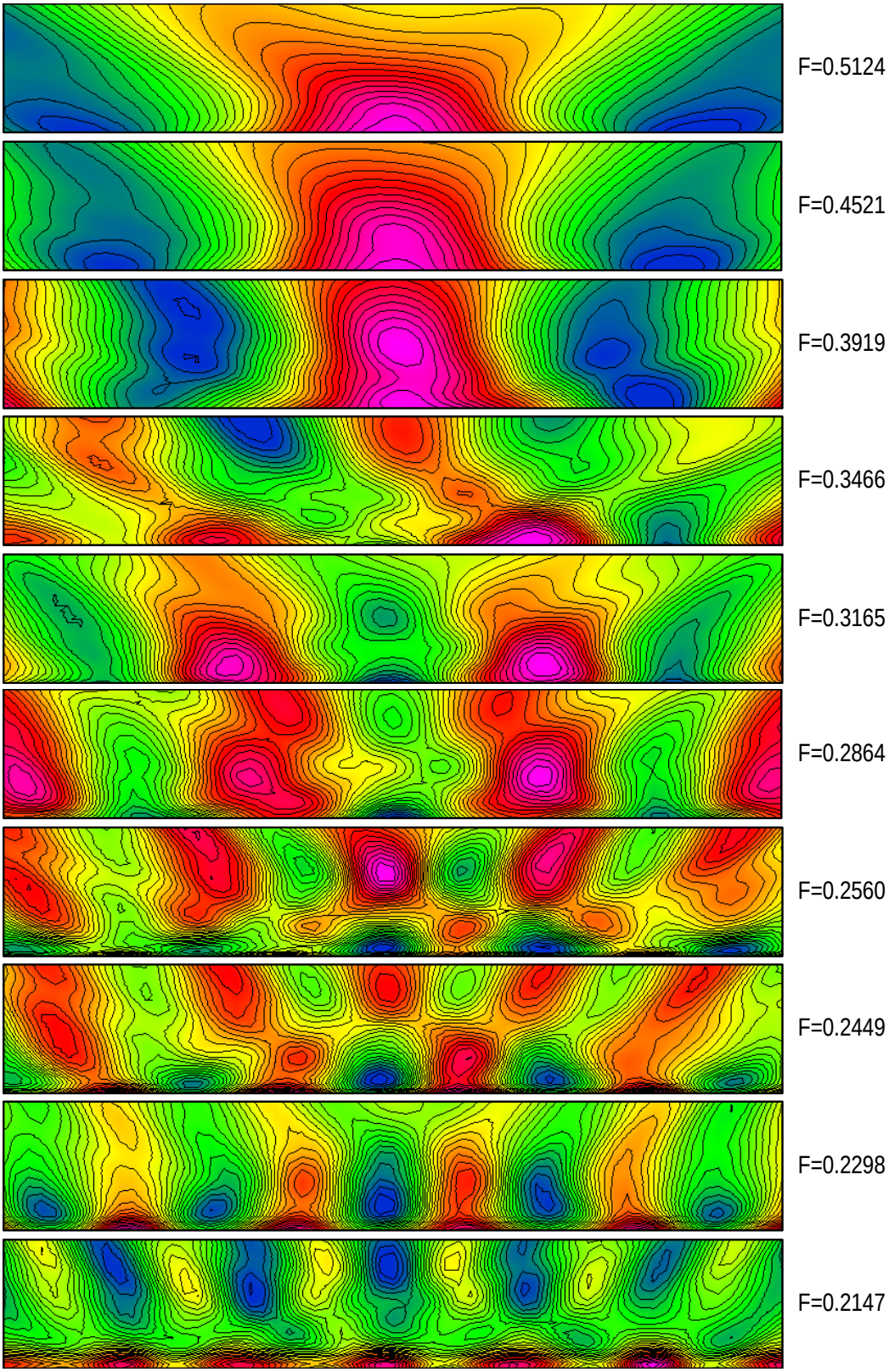

Fig. 3. Contour plots of wave drag coefficient $C_W(a,\ b)$ predicted by method 2 for 10 Froude numbers $(-0.75 \leq a \leq 0.75\ ,\quad 0.05 \leq b \leq 0.3)$

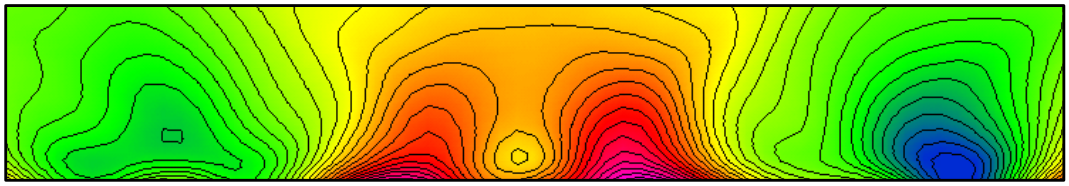

Fig. 4. Contour plot of wave drag coefficient (predicted by method 2) averaged over 38 Froude numbers $(-0.75 \leq a \leq 0.75\,, \quad 0.1 \leq b \leq 0.3)$

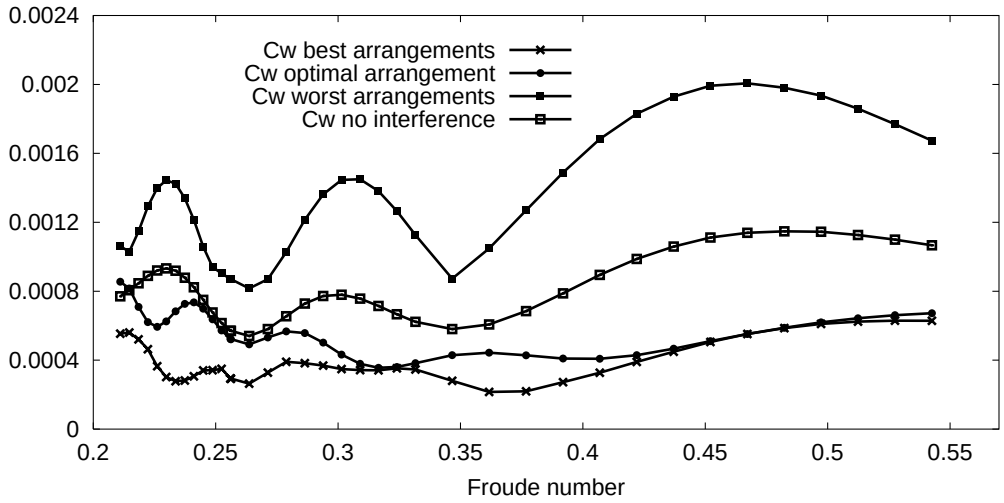

Fig. 5. Computed wave drag coefficient for different hull arrangements

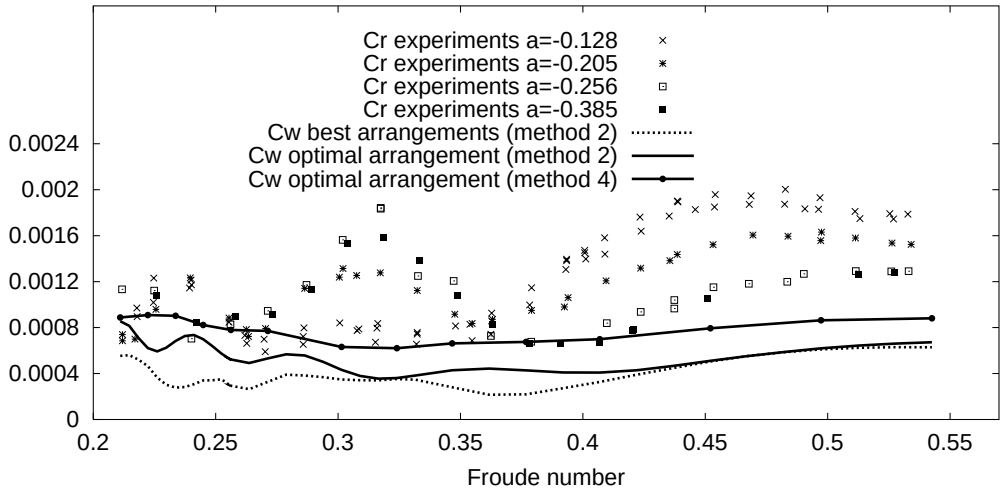

Fig. 6. Computed wave drag coefficient and experimental residuary drag coefficient for different hull arrangements

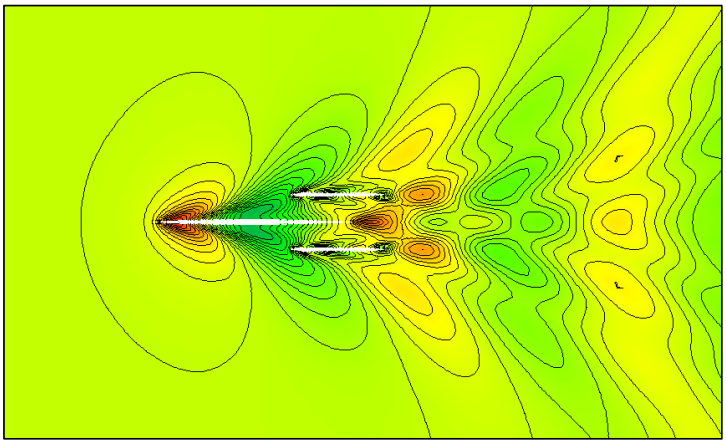

Best arrangement (a=-0.425, b=0.14, Cw=0.610e-3)

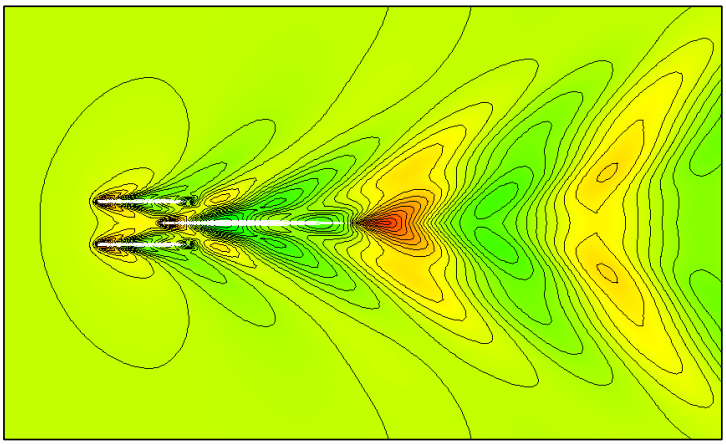

Optimal arrangement (a=0.575, b=0.11, Cw=0.699e-3)

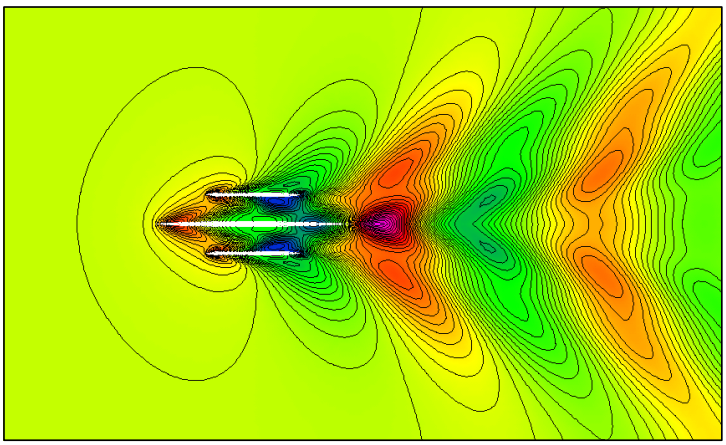

Worst arrangement (a=0., b=0.15, Cw=2.015e-3)

Fig. 7. Wave patterns predicted by method 4 for three hull arrangements at F=0.4069

CONCLUSION

Illustrative practical applications of CFD tools to the wave cancellation multihull ship concept examined in Wilson et al. (1993) and Yang et al. (2000) have been summarized. The trimaran considered in Wilson et al. (1993), Yang et al. (2000), and here consists of a main center hull and two identical outer hulls centered at $(x\,,y) = (a\,,\pm b)$ with respect to the center of the waterplane of the center hull. The elementary design problem of determining the optimal arrangement of the outer hulls with respect to the main center hull, i.e. the optimal values of the two parameters a and b, for the purpose of minimizing the wave drag of the ship has been considered using four methods of analysis.

One of the four methods is the near-field flow calculation method presented in Löhner et al. (1999) and Yang and Löhner (1998). This method is based on the Euler equations and the nonlinear free-surface boundary condition. The other three methods are linear potential flow methods that correspond to a hierarchy of simple approximations based on the Fourier-Kochin representation of ship waves and the slender-ship approximation given in Noblesse (2001,1983). These four methods of analysis have been compared to one another and to the experimental data given in Wilson et al. (1993) for the purpose of establishing and validating a practical methodology that can be used for more complex hull-form design problems involving minimization of ship drag.

In addition to the problem of selecting optimal hull arrangements considered here, a realistic trimaran design problem involves optimal selections of the lengths, beams, drafts, and shapes of the main center hull and the outer hulls, which have been taken as in Wilson et al. (1993) here for the purpose (of main interest for the present study) of comparing and validating alternative methods of analysis. Furthermore, constraints associated with mission requirements, structural considerations, seakeeping, and course keeping must evidently be considered.

The three methods based on the Fourier-Kochin representation of ship waves and the slender-ship approximation, especially the methods (called methods 1 and 2) corresponding to the zeroth-order and first-order slender-ship approximations given in Noblesse (1983), provide simple and highly efficient tools. These practical tools have been shown to be adequate for the purpose of determining optimal locations of the outer hulls. Method 4, based on a more refined flow analysis, can then be used effectively to further evaluate the flow at the optimal outer-hull arrangement.

The use of a pragmatic approach that relies on a combination of simple and more refined tools evidently is a well-established practice. In particular, the zeroth-order slender-ship approximation (i.e. method 1) has previously been used with success for hull-form optimization in Letcher et al. (1987) and Wyatt and Chang (1994). Thus, the practical usefulness of this remarkably simple approximation is confirmed in the present study, and in the companion studies of Percival and Noblesse (2001) and Hendrix et al. (2001).

ACKNOWLEDGEMENTS

The work of Yang and Löhner was partially funded by AFOSR (Dr. Leonidas Sakell technical monitor) and by NRL LCP&FD (Dr. William Sandberg technical monitor). Noblesse's work was supported by the ILIR program at NSWCCD. Computations were performed on a 128-Processor R10000 SGI Origin 2000 at NRL.

REFERENCES

D. Hendrix, S. Percival & F. Noblesse (2001) *Practical hydrodynamic optimization of a mononhull*, 2001 SNAME Annual Meeting, Orlando, FL

J.S. Letcher Jr., J.K. Marshall, J.C. Oliver III & Nils Salvesen (1987) *Stars & Stripes*, Scientific American 257: 34-40

R. Löhner, C. Yang, E. Oñate & S. Idelssohn (1999) *An unstructured grid-based, parallel free-surface solver*, Applied Numerical Mathematics 31: 271-293

F. Noblesse (1983) *A slender-ship theory of wave resistance*, Jl Ship Research 27: 13-33

F. Noblesse (2001) *Analytical representation of ship waves*, Ship Technology Research 48: 23-38

S. Percival & F. Noblesse (2001) *Experimental and theoretical evaluation of a series of hull forms*, 2001 SNAME Annual Meeting, Orlando, FL

M.B. Wilson, C.C. Hsu & D.S. Jenkins (1993) *Experiments and predictions of the resistance characteristics of a wave cancellation multihull ship concept*, 23rd American Towing Tank Conf., 103-112

D.C. Wyatt & P.A. Chang (1994) *Development and assessment of a total resistance optimized bow for the AE 36*, Marine Technology 31: 149-160

C. Yang & R. Löhner (1998) *Fully nonlinear ship wave calculation using unstructured grid and parallel computing*, 3rd Osaka Coll. Advanced CFD Applications to Ship Flow and Hull Form Design, Osaka, 125-150

C. Yang, R. Löhner & F. Noblesse (2000) *Farfield extension of near-field steady ship waves*, Ship Technology Research 47: 22-34

C. Yang, F. Noblesse, R. Löhner, D. Hendrix (2000) *Practical CFD applications to design of a wave cancellation multihull ship*, 23rd Symp. on Naval Hydro., Val de Reuil, France.